SAND96-1480C
CONF-9606247--1

GENERAL SOLUTIONS FOR THE OXIDATION KINETICS OF POLYMERS

Kenneth T. Gillen, Roger L. Clough and Jonathan Wise
Sandia National Laboratories
Albuquerque, NM 87185-1407, USA

ABSTRACT

The simplest general kinetic schemes applicable to the oxidation of polymers are presented, discussed and analyzed in terms of the underlying kinetic assumptions. For the classic basic autoxidation scheme (BAS), which involves three bimolecular termination steps and is applicable mainly to unstabilized polymers, typical assumptions used singly or in groups include (1) long kinetic chain length, (2) a specific ratio of the termination rate constants and (3) insensitivity to the oxygen concentration (e.g., domination by a single termination step). Steady-state solutions for the rate of oxidation are given in terms of one, two, three, or four parameters, corresponding respectively to three, two, one, or zero kinetic assumptions. The recently derived four-parameter solution predicts conditions yielding unusual dependencies of the oxidation rate on oxygen concentration and on initiation rate, as well as conditions leading to some unusual diffusion-limited oxidation profile shapes. For stabilized polymers, unimolecular termination schemes are typically more appropriate than bimolecular. Kinetics incorporating unimolecular termination reactions are shown to result in very simple oxidation expressions which have been experimentally verified for both radiation-initiated oxidation of an EPDM and thermoxidative degradation of nitrile and chloroprene elastomers.

INTRODUCTION

Oxidation of organic materials has been extensively studied for decades. The simplest and most commonly used kinetic schemes are based on various combinations of the reactions shown in Fig. 1. The first six reactions, comprising an initiation step, two propagation reactions and three bimolecular termination reactions constitute what is referred to as the basic autoxidation scheme (BAS), derived by Bolland [1], Bateman [2] and co-workers almost 50 years ago. This scheme is often assumed to be applicable to unstabilized materials at low to moderate temperatures. For stabilized materials, the presence of antioxidants (AH) often leads to a replacement of the three bimolecular reactions with the termination reactions 7 and 8. These two reactions are pseudo first-order (unimolecular) when the AH is present in high enough concentration such that it can be considered constant during the degradation. At high temperatures or for long times at intermediate temperatures, branching reactions (such as reaction 9) caused by the breakdown of ROOH species can enter.

The first objective of the present paper is to review our state of knowledge concerning solutions of the BAS, including our recent steady-state analysis which eliminates all simplifying

assumptions. The second objective is to briefly discuss unimolecular termination kinetic schemes and show that even in the presence of branching reactions, these schemes can result in simple, widely applicable oxidation expressions.

$$Polymer \xrightarrow{r_i} R\bullet$$
$$R\bullet + O_2 \xrightarrow{k_2} RO_2\bullet$$
$$RO_2\bullet + RH \xrightarrow{k_3'} RO_2H + R\bullet$$
$$R\bullet + R\bullet \xrightarrow{k_4} Products$$
$$R\bullet + RO_2\bullet \xrightarrow{k_5} Products$$
$$RO_2\bullet + RO_2\bullet \xrightarrow{k_6} Products + O_2$$
$$R\bullet + AH \xrightarrow{k_7} Products$$
$$RO_2\bullet + AH \xrightarrow{k_8} Products$$
$$RO_2H \xrightarrow{k_9} 2R\bullet + ROH + HOH$$

Figure 1. General reaction scheme for oxidation of polymers

RESULTS AND DISCUSSION- UNSTABILIZED POLYMERS

Steady-state BAS solution with one or more kinetic assumptions

The first six reactions shown in Fig. 1 constitute the basic autoxidation scheme (BAS), which is often assumed to be applicable to unstabilized polymeric materials. Without any assumptions, six parameters would be needed to fully describe this kinetic scheme. The number of necessary parameters is reduced to four by assuming that the concentrations $[R\bullet]$ and $[RO_2\bullet]$ quickly establish steady-state conditions, i.e.,

$$\frac{d[R\bullet]}{dt} = r_i - k_2[R\bullet][O_2] + k_3[RO_2\bullet] - 2k_4[R\bullet]^2 - k_5[R\bullet][RO_2\bullet] = 0 \quad (1)$$

$$\frac{d[RO_2\bullet]}{dt} = k_2[R\bullet][O_2] - k_3[RO_2\bullet] - k_5[R\bullet][RO_2\bullet] - 2k_6[RO_2\bullet]^2 = 0 \quad (2)$$

To proceed further, past analyses utilized one or more additional simplifying assumptions, further reducing the number of necessary parameters. The first assumption, utilized in the earliest papers [1,2], is that of long kinetic chain length, which implies that

$$k_2[R\bullet][O_2] = k_3'[RH][RO_2\bullet] = k_3[RO_2\bullet] \quad (3)$$

where, for convenience the concentration $[RH]$ is included in k_3. This assumption also implies that the rate of oxygen consumption is completely dominated by the second reaction (oxygen produced from reaction 6 is ignored) which leads to [1,2]

$$\frac{dO_2}{dt} = \left[\frac{1}{r_0^2} + \frac{1}{r_s^2} + \frac{\varphi}{r_0 r_s}\right]^{-0.5} \quad (4)$$

where the three parameters necessary for modeling the oxidation rate in eq. (4) are given by

$$r_0 = k_2(O_2)\sqrt{\frac{r_i}{2k_4}} \tag{5}$$

$$r_s = k_3\sqrt{\frac{r_i}{2k_6}} \tag{6}$$

$$\varphi = \frac{k_5}{\sqrt{k_4 k_6}} \tag{7}$$

A second assumption that is often used is that the three termination rate constants are related by $k_5^2 = 4k_4k_6$, equivalent to $\varphi = 2$. From eq. (4), this leads to

$$\frac{dO_2}{dt} = \frac{r_0}{1+\frac{r_0}{r_s}} = \frac{C_1[O_2]}{1+C_2[O_2]} \tag{8}$$

where this additional assumption now reduces the number of required parameters to two and the two constants for this bimolecular scheme are given by

$$C_{1b} = k_2\sqrt{\frac{r_i}{2k_4}} \tag{9}$$

$$C_{2b} = \frac{k_2}{k_3}\sqrt{\frac{k_6}{k_4}} \tag{10}$$

We label the constants C_1 and C_2 with subscripts b in eqs. (9) and (10) to emphasize that they refer to the simple theory for bimolecular termination. Later we will show that several unimolecular termination kinetic schemes lead to exactly the same functional dependence on $[O_2]$ shown in eq. (8), only differing in the values of the two constants C_1 and C_2.

The meaning of the parameters r_0 and r_s is clear if we evaluate eqs. (4) and (8) at the limits of low and high oxygen concentrations, since the rate of oxidation will equal r_0 at low oxygen concentrations and r_s at high (saturation) oxygen concentrations. In these limits, we have further reduced the number of required parameters to a single parameter, assuming that only termination reaction 4 is important in the low oxygen concentration limit and, similarly, that only termination reaction 6 is important in the high oxygen concentration limit.

The BAS has also been solved under steady-state conditions using the second assumption ($\varphi = 2$), but not the first (i.e., any kinetic chain length is allowed). The complicated result [3], which accounts for the oxygen produced in the sixth reaction of Fig. 1, can be expressed as

$$\frac{dO_2}{dt} = \frac{r_0(r_i+r_s)^2 + r_0^2\left(\frac{r_i}{2}+r_s\right)}{(r_i+r_s+r_0)^2} \tag{11}$$

For low and high oxygen concentrations, eq. (11) reduces to limits of r_0 and $(r_i/2) + r_s$, respectively.

General steady-state BAS solution (no assumptions)

Although a complete kinetic analysis of the BAS without any simplifying assumptions has been sought for more than 40 years, we know of no published account of success. In fact, some past workers have claimed that success was not possible without at least one simplifying assumption [4]. Recently, we were able to derive the first steady-state solution of the BAS without the necessity of invoking either of the two normally used assumptions [5]. Our approach was to first add the steady state relationships for $[R\bullet]$ and $[RO_2\bullet]$ given in eqs. (1) and (2) and solve the resulting quadratic equation for $[RO_2\bullet]$, yielding

$$\left[RO_2\bullet\right]=\frac{k_5}{2k_6}[R\bullet]\left[-1+\sqrt{1-\frac{4k_6k_4}{k_5^2}+\frac{2k_6r_i}{k_5^2[R\bullet]^2}}\right] \tag{12}$$

Instead of attempting to substitute this result back into eq. (1) and then solve for $[R\bullet]$ explicitly, which yields an equation in $[R\bullet]$ that is difficult to work with, we pursued a somewhat different approach. For notational convenience, we define

$$g=-1+\sqrt{1-\frac{4k_6k_4}{k_5^2}+\frac{2k_6r_i}{k_5^2[R\bullet]^2}}=-1+\sqrt{1-B+s} \tag{13}$$

By substituting eqs. (12) and (13) into eq. (1) and solving the resulting quadratic expression for $[R\bullet]$, we obtain

$$[R\bullet]=\frac{\frac{1}{4k_4}\left[k_2[O_2]-\frac{k_3k_5g}{2k_6}\right]}{1+\frac{k_5^2g}{4k_4k_6}}\left[-1+\sqrt{1+\frac{8r_ik_4\left[1+\frac{k_5^2g}{4k_4k_6}\right]}{\left[k_2[O_2]-\frac{k_3k_5g}{2k_6}\right]^2}}\right] \tag{14}$$

Since g contains $[R\bullet]$, eq. (14) is not an analytic, but rather an implicit solution for $[R\bullet]$. The utility of this approach depended on the fact that a self-consistent solution was shown to be possible since s (and therefore g) can be eliminated as an independent variable [5].

The final generalized solution to the BAS kinetic scheme for the rate of oxygen consumption is

$$-\frac{d[O_2]}{dt}=\frac{-k_2^2[O_2]^2(1-\rho)}{4k_4\left(1+\frac{g}{B}\right)}\left[-1+\sqrt{1+\frac{1}{\eta}}\right]\left[1-\frac{(1-\rho)g^2}{4B\left(1+\frac{g}{B}\right)\left(-1+\sqrt{1+\frac{1}{\eta}}\right)}\right] \tag{15}$$

where the parameter η is given by

$$\eta=\frac{k_2^2[O_2]^2(1-\rho)^2}{8r_ik_4\left[1+\frac{g}{B}\right]} \tag{16}$$

and the parameter ρ, given by

$$\rho = \frac{k_3[RO_2\bullet]}{k_2[R\bullet][O_2]} = \frac{\frac{k_3 k_5 g}{2k_6}}{k_2[O_2]} \tag{17}$$

is related to the kinetic chain length and takes on values ranging from 0 (zero kinetic chain length) to 1 (long kinetic chain length).

The generalized solution shown in eq. (15) contains four independent parameters, B, η, ρ and $k_2^2[O_2]^2 / 4k_4$ (g is a known parameter once B and η are specified). The generalized model parameter $B = 4k_4k_6 / k_5^2$ can now be set equal to any value, thereby relaxing the assumption of the simplified model that it is equal to unity. The parameter ρ, which is related to the kinetic chain length, represents the relaxation of the second, often-used simplifying assumption of long kinetic chain length. Although the parameter η, defined in eq. (16), involves a complex mixture of B, ρ and several rate constants, it mainly reflects the oxygen concentration dependency. At sufficiently large values of η, the oxidation rate given by eq. (15) will become independent of oxygen concentration.

Kinetic chain length

The traditional definition of kinetic chain length (kcl) is the number of oxygen molecules consumed per initiation step, which is only valid under the assumption of long kcl, where the oxygen produced from reaction 6 can be ignored. A better definition that holds for all values of kcl is the number of RO_2H molecules formed per initiation step, which means that

$$kcl = \frac{k_3[RO_2\bullet]}{r_i} \tag{18}$$

In terms of the analysis that led to eq. (11), where the long kcl assumption was relaxed but ϕ was assumed to be equal to 2 (equivalent to B being equal to 1), eq. (18) leads to

$$kcl = \frac{r_0 r_s}{r_0 + r_s + r_i} \tag{19}$$

For the completely generalized analysis, eq. (18) can be shown to yield [5]

$$kcl = \frac{\rho}{1-\rho}\left[2\eta\left(-1+\sqrt{1+\frac{1}{\eta}}\right)\right] \tag{20}$$

Results based on eq. (20) are plotted in Fig. 2, where it is seen that small to moderate values of kcl correspond to values of ρ in the range of ~0.1 to 0.95.

Dependence on initiation rate

For experimental testing of oxidation models, two of the parameters that are most easily controlled are the oxygen concentration $[O_2]$ and the initiation rate, r_i. We will briefly discuss the predicted dependencies on the initiation rate in this section and on the oxygen concentration in the following section. For the simplest theory, eqs. (8) and (9) show that the oxidation rate is

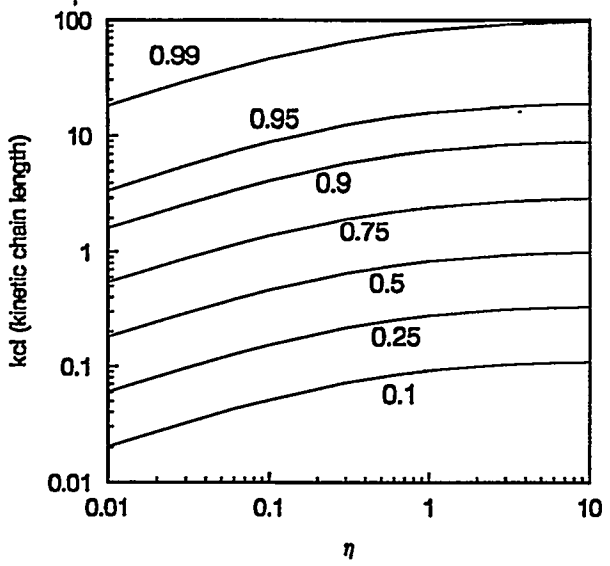

Fig. 2. The kinetic chain length, as defined by eq. (20), versus η at the indicated values of ρ.

predicted to depend on the square root of the initiation rate. For the completely generalized model, we obtain

$$\frac{\left(\frac{dO_2}{dt}\right)}{\left(\frac{dO_2}{dt}\right)_r} = \frac{(1-\rho)(B+g_r)\left[-1+\sqrt{1+(1/\eta)}\right]\left[1-\frac{(1-\rho)g^2}{4(B+g)}\left(-1+\sqrt{1+(1/\eta)}\right)\right]}{(1-\rho_r)(B+g)\left[-1+\sqrt{1+(1/\eta_r)}\right]\left[1-\frac{(1-\rho_r)g_r^2}{4(B+g_r)}\left(-1+\sqrt{1+(1/\eta_r)}\right)\right]} \tag{21}$$

where the subscripts r denote the values of the parameters under reference initiation conditions. An iterative calculation approach is used to determine the values of the parameters at a given selected multiplicative increase in the initiation rate. Some representative results are shown in Figs. 3 and 4. Figure 3 shows the predicted dependence versus ρ for $\eta_r = 100$ and $B = 1$,

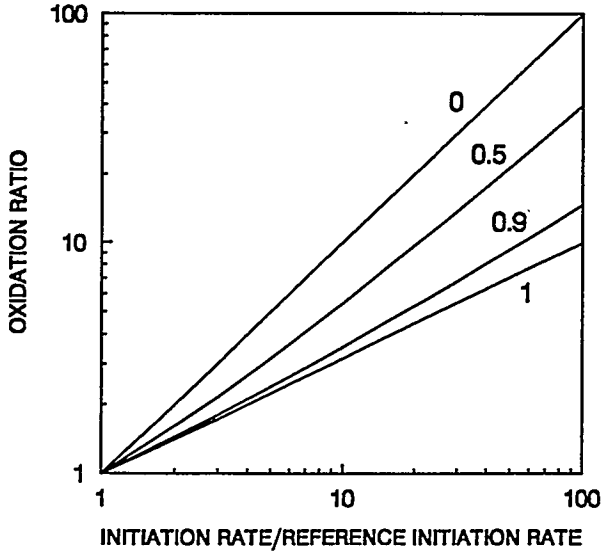

Fig. 3. Effect on the oxidation rate of increasing the initiation rate relative to its reference conditions when $B = 1$, $\eta_r = 100$, and ρ_r takes on the indicated values.

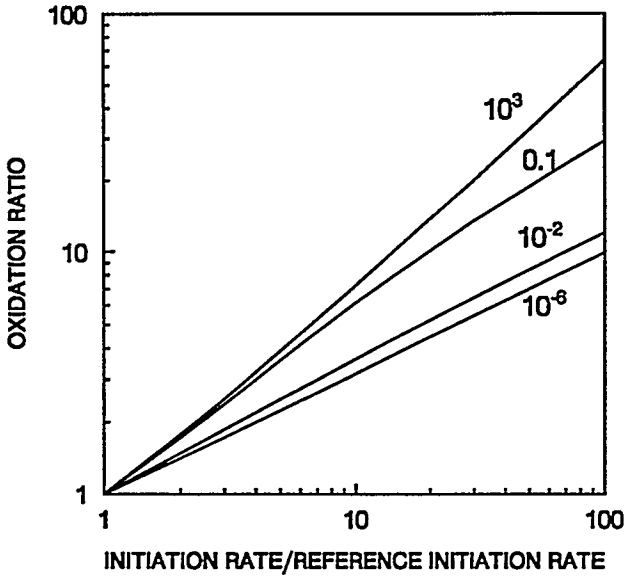

Fig. 4. Effect on the oxidation rate of increasing the initiation rate relative to its reference conditions when $B = 10^{-6}$, $\rho_r = 0.25$, and η_r takes on the indicated values.

thereby corresponding to the relaxation of only one of the two usual assumptions. If we define the dependence as r_i^n, then n varies from 0.5 (as expected) for long kcl ($\rho = 1$) to 1.0 at zero kcl ($\rho = 0$). The deviations from an n of 0.5 are greatest for large values of η_r, which correspond to oxidation conditions that are insensitive to oxygen concentration. The effects shown become less pronounced for lower values of η_r, where the oxidation rate depends on the oxygen concentration. Figure 4 shows some representative results versus values for η_r, when both of the normal assumptions are simultaneously relaxed ($B = 10^{-6}$ and $\rho_r = 0.25$). These and similar results under other conditions allow us to conclude that the presence of low to intermediate kcl can be used to explain the often-observed non square-root dependence on the initiation rate.

Dependence on oxygen concentration

For the simplest theory, eq. (8) shows that the oxidation rate is expected to be linearly dependent (slope of 1) on oxygen concentration at low oxygen concentrations. Once the oxygen concentration reaches a certain level, the slope begins to decrease continuously until it asymptotically approaches a slope of zero at high oxygen concentrations. Very different results can occur for the other models. For the most general model [5],

$$\frac{\left(\frac{dO_2}{dt}\right)}{\left(\frac{dO_2}{dt}\right)_r} = Y^2 \frac{(1-\rho)(B+g_r)\left[-1+\sqrt{1+(1/\eta)}\right]\left[1-\frac{(1-\rho)g^2}{4(B+g)}\left(-1+\sqrt{1+(1/\eta)}\right)\right]}{(1-\rho_r)(B+g)\left[-1+\sqrt{1+(1/\eta_r)}\right]\left[1-\frac{(1-\rho_r)g_r^2}{4(B+g_r)}\left(-1+\sqrt{1+(1/\eta_r)}\right)\right]} \qquad (22)$$

where the subscripts r denote the values of the parameters under reference oxygen concentration conditions and Y is the multiplicative increase in the oxygen concentration relative to reference conditions. Again, an iterative calculation approach is used to determine the values of the parameters under the increased oxygen concentration conditions. Figure 5 shows some representative results for various values of B when $\eta_r = 0.1$ and $\rho_r = 0.75$, conditions which correspond to a moderate kcl, as seen from Fig. 2. Especially interesting behavior occurs for

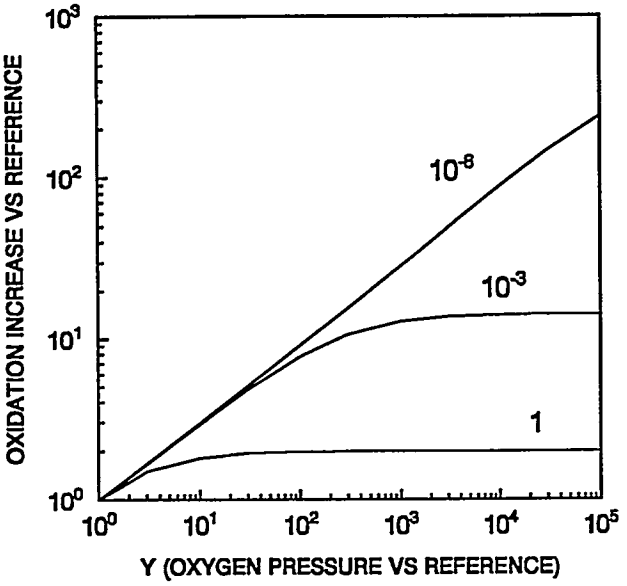

Fig. 5. Effect on the oxidation rate of increasing the oxygen concentration by a factor *Y* above its reference value for the generalized theory when $\eta_r = 0.1$, $\rho_r = 0.75$, and *B* takes on the indicated values.

small values of *B*, where the oxidation rate can remain proportional to the square root of the oxygen concentrations for many decades of increase in oxygen concentration. Similar behavior can occur for the modeling that assumes long kcl, but relaxes the assumption that φ=2. This is clear from examining eq. (4) for large values of φ (equivalent to small values of *B*), where the equation predicts a square root dependence on oxygen concentration.

Diffusion-limited oxidation profile shape analyses

If oxidation dominates the degradation of a polymeric material and the rate of oxygen consumption is greater than the rate at which dissolved oxygen can be resupplied to the interior of the material by diffusion from the surrounding atmosphere, more oxidation will occur near the surfaces than in the interior. This phenomenon, referred to as diffusion-limited oxidation, is extremely common under laboratory aging conditions and leads to heterogeneously oxidized materials. The resulting oxidation profiles can be measured experimentally by various methods and modeled theoretically by combining oxidation rate expressions with diffusion equations. Cunliffe and Davis [6] showed how this could be accomplished for the simplest oxidation model given in eq. (8). Their steady state result for a sheet of material of thickness *L* depended on two parameters, α and β, given by

$$\alpha = C_1 \frac{L^2}{D} \qquad \text{and} \qquad \beta = C_2 S p = C_2 \left[O_2\right]_r \tag{23}$$

where *S* and *D* are the solubility and diffusion parameters for oxygen in the material, *p* is the oxygen partial pressure surrounding the sample and $\left[O_2\right]_r$ is the reference or equilibrium dissolved oxygen concentration at the sample surface. Figure 6 shows example profiles derived from this modeling. For small values of β, which correspond to the oxygen pressure region where the oxidation is linearly related to oxygen concentration, the profiles are "U-shaped". For large values of β, which correspond to the oxygen saturation region, "step-like" drop-offs in oxidation can occur for thick enough samples (high enough values of α). Behavior between

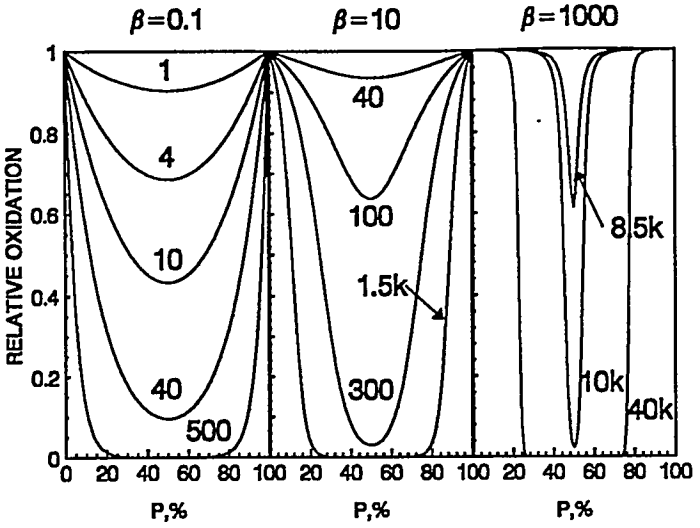

Fig. 6. Theoretical oxidation profiles for the simplest BAS theory for the three indicated values of β at various values of α. P is the percentage of distance across the sample cross-section.

these extremes occurs for intermediate values of β. It was also shown that the following additional relationship holds [6]

$$\frac{\left(\frac{dO_2}{dt}\right)_r L^2}{pP_{ox}} = \frac{\alpha}{\beta+1} \tag{24}$$

where P_{ox}, the oxygen permeability coefficient, is the product of S and D. Since the oxygen consumption rate and the oxygen permeability coefficient can be measured, this relationship can be used to test theoretical fits of experimental profile data.

For the most general model of oxidation, corresponding to eq. (15) above, theoretical diffusion-limited oxidation profiles for a sheet of material of thickness L are obtained [5] as a function of three of the model variables, η, ρ and B plus a fourth thickness dependent variable χ defined by

$$\chi = \frac{k_2^2 L^2 (1-\rho)\left[O_2\right]_r}{4k_4 D\left(1+\frac{g}{B}\right)} \tag{25}$$

In general, the profile shapes versus the four theoretical parameters behave similarly to those shown above for the simplest model, proceeding from "U-shaped" profiles at low values of η (low oxygen concentration limit) to "step-like" drop-offs at high values of η (oxygen saturation). Some unusual behavior occurs for small values of B when η is close to 1 (an intermediate value of this parameter). In such instances, approximately linear drop-offs can occur under long kcl (high ρ) conditions, as shown in Fig. 7. Even more interesting profile shapes can occur for small values of B and values of η close to 1 when both simplifying assumptions are relaxed, as shown in Fig. 8.

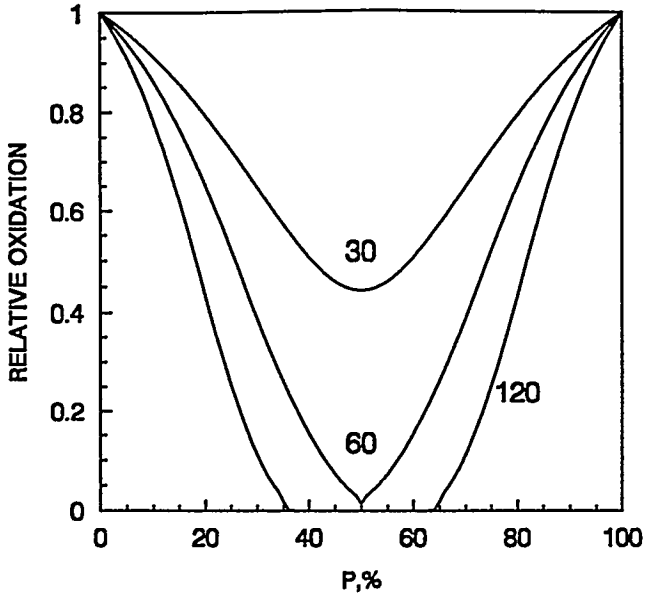

Fig. 7. Theoretical oxidation profiles for $\eta = 1$, $\rho = 0.95$, $B = 10^{-6}$ and the indicated values of χ.

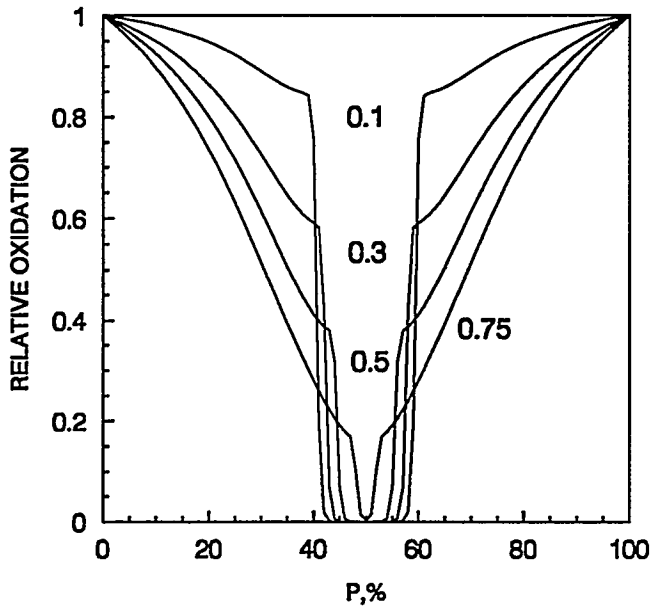

Fig. 8. Theoretical oxidation profiles for $\chi = 50$, $\eta = 1$, $B = 10^{-6}$ and the indicated values of ρ.

In analogy with eq. (24) for the simplest model, a potentially useful governing relationship for the generalized model is [5]

$$\frac{\left(\frac{dO_2}{dt}\right)_r L^2}{pP_{ox}} = \chi_r\left[-1+\sqrt{1+\frac{1}{\eta_r}}\right]\left[1-\frac{(1-\rho_r)g_r^2}{4(B+g_r)}\left(-1+\sqrt{1+\frac{1}{\eta_r}}\right)\right] \qquad (26)$$

If experimental diffusion-limited profiles can be obtained together with estimates of the oxygen permeability coefficient, theoretical fits constrained by eq. (26) together with measurements of

oxidation rates versus initiation rate and oxygen concentration should allow the four generalized BAS model parameters to be estimated.

RESULTS AND DISCUSSION- STABILIZED POLYMERS

Steady-state unimolecular solutions

For many stabilized polymers, a more appropriate kinetic scheme replaces the three bimolecular termination reactions with the two pseudo unimolecular termination reactions shown as reactions 7 and 8 in Fig. 1. Without branching, the steady-state solution for the oxidation rate with unimolecular termination is given by an equation identical to eq. (8) except for the values of C_1 and C_2, which are given by [7]

$$C_{1u} = \frac{r_i k_2}{k_7} \quad \text{and} \quad C_{2u} = \frac{k_2 k_8}{k_7 (k_3 + k_8)} \tag{27}$$

where the subscript u refers to the simplest unimolecular case.

Even with branching reactions (reaction 9 in Fig. 1), as long as the RO_2H concentration reaches a steady state, eq. (8) again describes the oxidation rate except that the values of C_1 and C_2 are now given by [8]

$$C_{1ub} = \frac{r_i k_2}{k_7} \quad \text{and} \quad C_{2ub} = \frac{k_2 (k_8 - 2k_3)}{k_7 (k_3 + k_8)} \tag{28}$$

where the subscript ub refers to the unimolecular with branching case.

Since eq. (8) is therefore valid for both of these unimolecular cases as well as the simplest bimolecular case, all three cases would be predicted to have similar dependencies on the oxygen concentration. There are, however substantial differences in the predicted dependence on r_i, the initiation rate. For the unimolecular termination cases, eqs. (27) and (28) show that a first order behavior is expected, whereas eq. (9) predicts a square root dependence (half order) for the bimolecular case.

Experimental verification of simplest unimolecular model (no branching)

To test the simplest unimolecular oxidation model (no branching reactions), we carried out a careful study of a commercial (stabilized) EPDM seal material utilizing gamma radiation at various dose rates in order to control the initiation rate [7]. For this material, density changes were found to be proportional to the amount of oxidation and were therefore used to quantify the amount of oxidation. Although diffusion-limited oxidation effects were important under our aging conditions, we were able to use the surface density changes as a means of testing the dependence of oxidation rate on the dose rate (initiation rate). Results shown in Fig. 9 plotted versus total dose show that dose rate effects are absent for dose rates ranging from 6.65 kGy/h to 0.16 kGy/h! These data offer striking evidence for unimolecular (first order) behavior. Additional evidence came from oxygen consumption rate results which were independent of total dose for dose rates ranging from 0.12 kGy/h to 2.08 kGy/h.

To test the unimolecular diffusion-limited oxidation theory, we obtained experimental density profiles versus sample thickness, radiation dose rate and surrounding oxygen partial pressure. The resulting profile shapes and magnitudes were quantitatively fit with the two-

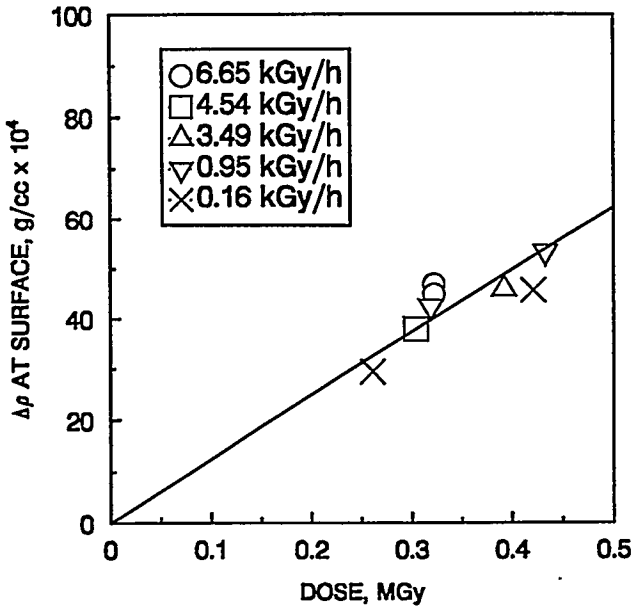

Fig. 9. Changes in density at the air-exposed surface of various samples of the EPDM material versus radiation dose at the indicated dose rates.

parameter (see eq. 23) theory based on the oxidation rate being described by eq. (8). Because first order behavior was confirmed, the proper C_1 functionality as given in eq. (27) was used to obtain the correct dependence on dose rate. Under ambient air conditions, the best fits occurred for β of 10, implying that the oxidation rate is within approximately 10% of its saturation value. Figure 10 shows an example of some of the experimental results together with the theoretical

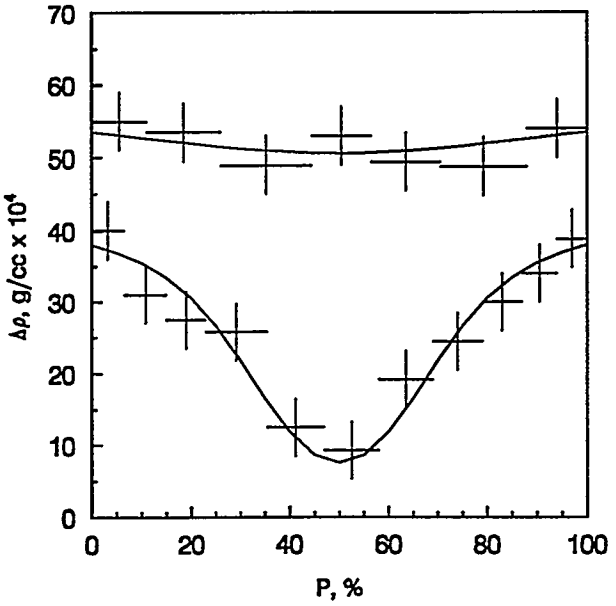

Fig. 10. Experimental profiles of density increases caused by radiation-induced oxidation of EPDM (crosses)- top data are for a 3.07 mm thick sample aged to 304 kGy at 4.54 kGy/h, bottom data are for a 3.02 mm thick material aged to 433 kGy at 0.95 kGy/h. The curves through the data are theoretical fits using $\beta = 10$ and $\alpha = 35.7$ (top) and 177 (bottom).

fits. After obtaining estimates of the model parameters α and β plus measurements of the oxygen permeability coefficient, we were able to show that these results were in accordance with the governing theoretical relationship given in eq. (24). This test represented further confirmation of the applicability of the simple unimolecular scheme to this material.

Experimental verification of unimolecular model with steady-state branching

Further testing of the unimolecular scheme involved air-oven aging studies of stabilized nitrile and neoprene elastomers [8,9]. For these materials, we followed various properties, including the oxygen consumption rate versus aging time and temperature. Figure 11 shows

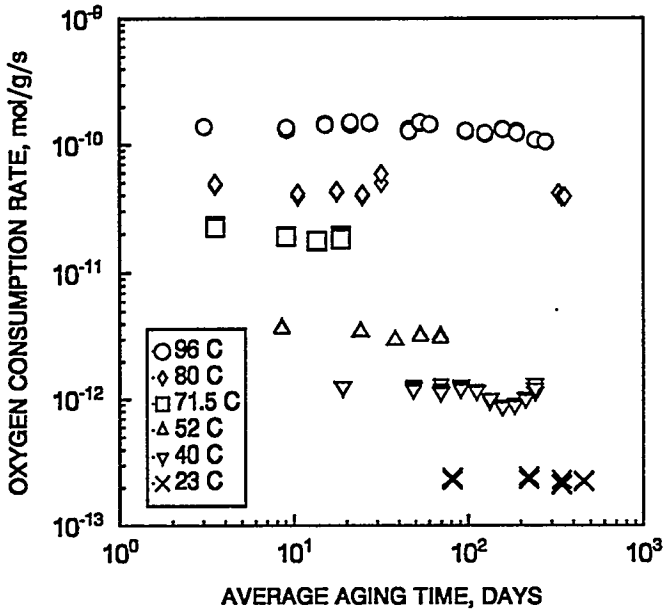

Fig. 11. Oxygen consumption rates for nitrile rubber material versus time at the indicated temperatures.

oxygen consumption rate results for the nitrile material at temperatures ranging from 96°C to ambient room temperature. Since mechanical property lifetimes (defined as the time required for the tensile elongation to decrease to 10% of its initial value) at 96°C and 80°C are approximately 100 days and 250 days, respectively, it is clear from this figure that the oxidation rate is approximately constant throughout the mechanical property lifetime. Similar results were observed for the neoprene material. Since we expected branching reactions to be important for these materials during thermoxidative aging, the observation of constant oxygen consumption implies that the RO_2H species responsible for the branching reactions have reached steady-state conditions. We therefore assumed that eq. (8) was appropriate together with the values of C_1 and C_2 given in eq. (28). By measuring the consumption rate versus oxygen partial pressure, we estimated that the β parameter in eq. (23) was approximately unity for air-aging of these materials. Finally, we were able to use this result to show that we could obtain essentially quantitative agreement between experimental diffusion-limited oxidation profiles and the theoretical profiles based on unimolecular modeling, as seen in Fig. 12.

ACKNOWLEDGMENT

This work was performed at Sandia National Laboratories and supported by the U. S. Department of Energy under Contract No. DE-AC04-94AL85000.

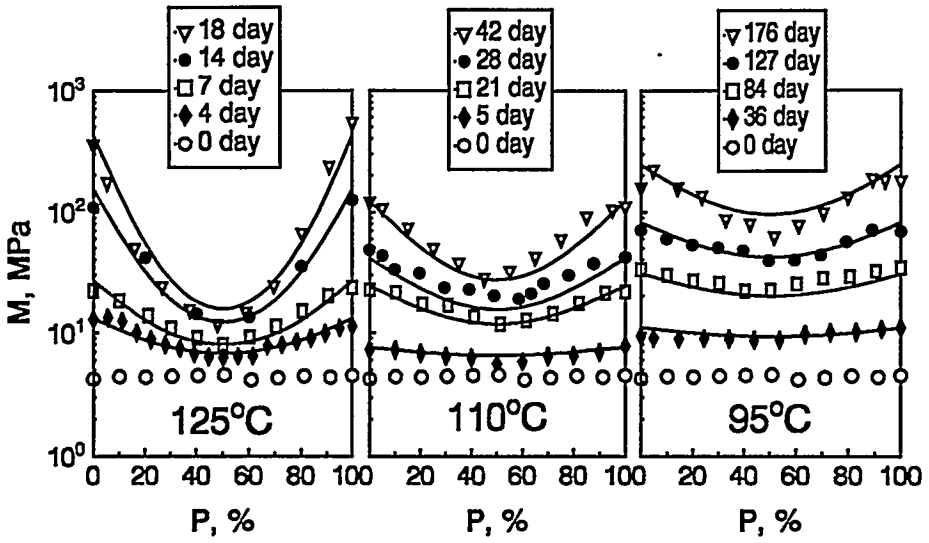

Fig. 12. Modulus profiles (symbols) versus temperature and time for 2 mm thick nitrile rubber samples plus theoretical predictions (curves) for the profiles.

REFERENCES

1. Bolland, J. L. *Proc. Roy. Soc.*, **A186** (1946) 218.
2. Bateman, L., *Q. Rev. (London)*, **8** (1947) 147.
3. Gorelik, B. A., Goldberg, V. M., Ivanov, A. I. & Semenenko, E. I., *Vysokomol. Soedin., Ser. B.*, **21** (1979) 298.
4. Uri, N., in *Autoxidation and Antioxidants, Vol. 1*, ed. W. O. Lundberg. Interscience Publishers, New York, 1961, p. 74.
5. Gillen, K. T., Wise, J. and Clough, R. L., *Polym. Deg. Stab.*, **47** (1995) 149.
6. Cunliffe, A. & Davis, A., *Polym. Deg. Stab.*, **4** (1982) 17.
7. Gillen, K. T. & Clough, R. L., *Polymer*, **33** (1992) 4358.
8. Wise, J., Gillen, K. T. and Clough, R. L., *Polym. Deg. Stab.*, **49** (1995) 403.
9. Wise, J., Gillen, K. T. and Clough, R. L., *Polymer*, in press.